1991

Critical fields and Landau-Ginzburg parameters of the heavy-fermion superconductor UPt_3

Zuyu Zhao
Northwestern University

F. Behroozi
Northwestern University

Shireen Adenwalla
University of Nebraska-Lincoln, sadenwalla1@unl.edu

Y. Guan
Northwestern University

J. B. Ketterson
Northwestern University

RAPID COMMUNICATIONS

PHYSICAL REVIEW B VOLUME 43, NUMBER 16 1 JUNE 1991

Critical fields and Landau-Ginzburg parameters of the heavy-fermion superconductor UPt_3

Zuyu Zhao, F. Behroozi,* S. Adenwalla, Y. Guan, and J. B. Ketterson
Department of Physics and Astronomy, Northwestern University, Evanston, Illinois 60208

Bimal K. Sarma
Department of Physics, University of Wisconsin at Milwaukee, Milwaukee, Wisconsin 53201

D. G. Hinks
Material Science Division, Argonne National Laboratory, Argonne, Illinois 60439
(Received 8 February 1991)

Measurements of both the lower and upper critical fields along all three principal axes of the heavy-fermion superconductor UPt_3 have been performed. A kink in the temperature dependence of the lower critical field, H_{c1}, is observed for all three orientations, which is in agreement with a recent theory by Hess, Tokuyasu, and Sauls. Also, an anisotropy of the temperature dependence of the lower critical field is observed at low temperatures ($T < 290$ mK). The Landau-Ginzburg parameters are estimated from the experimental results.

There is mounting experimental evidence that the superconducting state in the heavy-fermion material UPt_3 is of an unconventional nature with a multicomponent order parameter. Ultrasonic measurements[1-3] have revealed the presence of more than one superconducting state in the H-T plane, which has been corroborated by a variety of other measurements.[4] Heat-capacity data[5,6] show that multiple phases exist, even at zero field. Data on neutron scattering[7] indicate weak antiferromagnetic ordering at ~ 5 K, which may give rise to an interaction of magnetic and superconducting order parameters. Recently, Adenwalla *et al.*[8] have obtained a complete phase diagram in the H-T plane from longitudinal ultrasonic velocity measurements which confirm the existence of several superconducting phases.

Hess, Tokuyasu, and Sauls (HTS) have proposed[9] a model for the superconducting states of UPt_3 in which a two-dimensional order parameter gives rise to two superconducting phases of different symmetry existing in adjacent temperature domains. This is consistent with the presence of two jumps observed in the specific heat.[5,6] The model predicts an abrupt change in the slope of the upper critical field (H_{c2}) when the field is in the basal plane, due to the transition between two superconducting phases at some finite field. In addition, the lower critical field (H_{c1}) should display a kink for all field orientations at the temperature of the lower heat-capacity jump.

With an rf resonance technique which probes only the surface of the sample (about a London depth below T_c), Shivaram, Gannon, and Hinks[10] reported a kink in H_{c1} with the field along the a axis. No kink was observed for the field along the c axis. We mention in passing that the rf penetration data must be interpreted with caution, since the surface impedance of a nonconventional superconductor may show unusual behavior.

Here we present new lower-critical-field data which show a discontinuity of slope for all principal field orientations (a, b, and c), in conformity with the predictions of the HTS model. Our data are obtained from low-field dc magnetization curves of a single-crystal spherical sample of UPt_3. We emphasize here that, in order to obtain the lower critical fields reliably, it is essential to perform the magnetization measurements on a single-crystal ellipsoidal sample, which has a well-defined demagnetizing factor. Only an ellipsoidal sample gives rise to a uniform internal field when placed in a uniform external field. A spherical sample is perhaps the most convenient for magnetization measurements, since its demagnetizing factor is $\frac{1}{3}$ for all orientations.

Three samples were cut from a high-quality single-crystal ingot of UPt_3. The annealing process was optimized to yield the highest superconducting transition temperature, T_c, consistent with the sharpest transition. The ultrasonic attenuation[3] and velocity[8] measurements were performed on the first sample. A rudimentary zero-field heat-capacity measurement was performed on the second sample, and showed some indication of a double heat-capacity jump. The third sample was machined into a sphere [(4.03 ± 0.01) mm in diameter] by spark erosion, after which it was chemically etched and reannealed. As there was no significant change in T_c or the transition width, one may conclude that the quality of the spherical sample was comparable to the other two.

The measurements of the lower critical fields were performed with a quasistatic technique described elsewhere.[11] Basically, it involves integrating the signal from a balanced pair of pickup coils, one containing the sample, as the magnetic field is slowly ramped. The measurements were done on an Oxford 400 TLE dilution refrigerator modified to permit top loading of samples into the magnetometer.

The magnetometer consisted of a primary coil (for ac susceptibility measurements) and a pair of astatic secondary coils (for both ac and dc susceptibility measurements) wound on a leak-tight epoxy former. An rf coil located between the two secondaries formed part of a LC resonant circuit; the precise location of the UPt_3 sphere could be obtained by monitoring the frequency shift when

the sample was positioned at the rf coil center.

A carbon-resistance thermometer (Matsushita 100 Ω) was installed inside the epoxy former, which was calibrated *in situ,* at zero field, against a precalibrated germanium-resistance thermometer that was top loaded in a separate run. Reliable thermal contact between the sample, thermometer, and the mixing chamber was achieved by filling the epoxy former with liquid ^{3}He. The Matsushita carbon resistors have a very small magnetoresistance at these temperatures, as verified in a separate run. The maximum correction in temperature is of the order of 1% in the field range 0–3 T, corresponding to a $\Delta T < 5$ mK. This correction need only be applied for the H_{c2} measurements.

The residual field, usually encountered when a superconducting magnet has been previously energized, can become a serious problem when performing low-field measurements (such as H_{c1} in UPt_3). To solve this problem, the magnet was operated only at fields below 200 G (well below the lower critical field of the Nb-Ti windings) until all the desired low-field data were collected.

When the external field is ramped (at a constant rate), the net emf from the two "secondary" coils is proportional to the dc susceptibility of the sample.[11] Direct integration of this signal gives the magnetization (irrespective of the ramp rate).

Typically the low-field magnetization data were taken by warming the sample above T_c in zero field (to drive off any flux trapped in the sample) followed by cooling to a fixed temperature. The field was then ramped up at the rate of 1 G/sec to obtain the low-field magnetization data.

A typical trace taken at $T=230$ mK is shown in Fig. 1. The measured lower critical field of the sphere, referred to as $(H_{c1})_{\text{sphere}}$, is taken as the field at which the slope of the magnetization curve just begins to deviate from the linear Meissner value; the lower critical field is then given by

$$H_{c1} = \tfrac{3}{2}(H_{c1})_{\text{sphere}} . \quad (1)$$

Data were taken along all three principal axes of hexagonal UPt_3. The results can be summarized as follows: Figure 2(a) shows the lower critical fields as a function of temperature for the field parallel to the c axis, while Fig. 2(b) shows the data for the field parallel to the a and b axes. In all cases, a kink near 392 mK is fairly apparent. No difference in the H_{c1} data was observed with **H** parallel to the a or b axis, depicted respectively as the solid and open circles in Fig. 2(b). The error bar of our experimental data is approximately twice the size of the symbols in these two figures.

The straight lines for the combined a and b axes data [Fig. 2(b)] were fitted by the following procedure. The data were partitioned into low and intermediate field groups and separately fitted to straight lines. The total rms error was then minimized as a function of the partitioning point. This fitting gives the temperature of the kink, T_c^* [defined in Fig. 2(b)], as 385 mK. The ratio of the slopes of the H_{c1}-vs-T curve above and below T_c^* for the field in the basal plane is estimated to be $R_a = R_b = 1.19$.

When the external field was applied along the c axis [see Fig. 2(a)], the lower critical field displayed some curvature at temperatures close to T_c and far below T_c^*. For

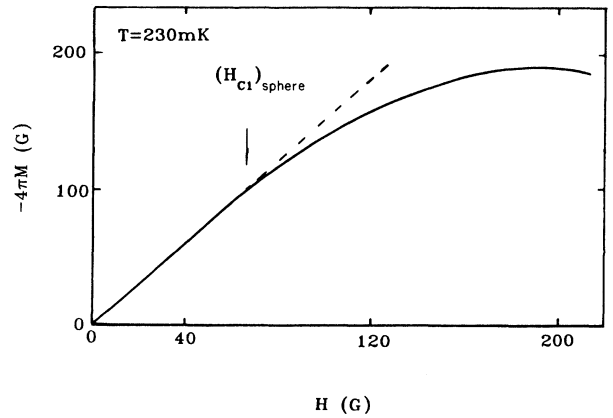

FIG. 1. A typical magnetometer trace taken at $T=230$ mK.

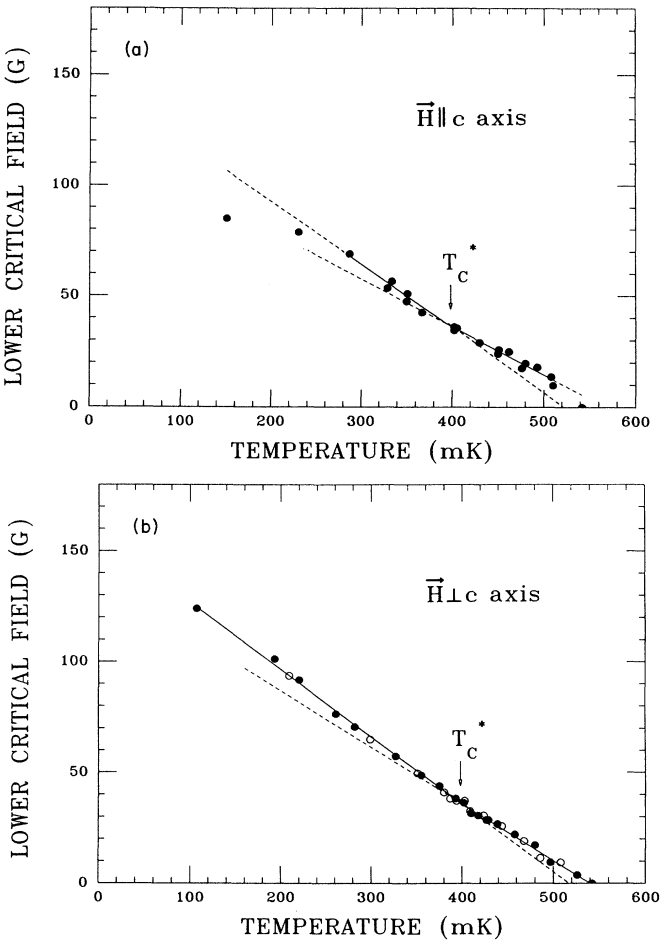

FIG. 2. (a) The lower critical fields vs temperature for **H**$\|c$. The solid circles and the straight lines are respectively the experimental data and the results of a linear least-squares fit (see text). (b) The lower critical fields vs temperatures for **H**$\perp c$. The solid (open) circles are the experimental data taken with **H**$\|a$ (b) axis. The straight lines are a linear least-squares fit (see text).

consistency, the same fitting procedure used for $\mathbf{H}\perp c$ was applied to $\mathbf{H}\parallel c$ data, but within the narrower temperature range, 290–510 mK [depicted in Fig. 2(a) with the solid lines]. This fit for $\mathbf{H}\parallel c$ axis gave $T_c^*=388$ mK and $R_c=1.28$. Although the fitting procedure used will, by construction, yield a numerical prediction for the kink temperature, the fact that the numerical values are nearly identical for all three orientations increases the confidence level of the method.

Another noteworthy feature of the lower critical field is its anisotropy at low temperatures. It is clear from Figs. 2(a) and 2(b) that no evident anisotropy is observed at temperatures $T>290$ mK (in agreement with the results of Vincent *et al.*[12]) However, when the sample was cooled below 290 mK, $-dH_{c1}/dT|_{\mathbf{H}\perp c\text{ axis}}$ remains unchanged, while $-dH_{c1}/dT|_{\mathbf{H}\parallel c\text{ axis}}$ decreases below 290 mK and H_{c1} saturates.

Since the HTS model predicts a kink in the H_{c1} curve for all directions, a discussion of our data in terms of this model may prove useful. According to the HTS theory, the ratio of the fourth-order parameter, $\beta=\beta_2/\beta_1$, and the ratio of the gradient coefficients, κ_1/κ_{123} (where $\kappa_{123}\equiv\kappa_1+\kappa_{23}$), can be expressed as follows:

$$T_c^*=\frac{T_c^+ + T_c^-}{2}\left(1-\frac{\beta_1}{\beta_2}\frac{T_c^+ - T_c^-}{T_c^+ + T_c^-}\right), \tag{2}$$

$$R_a=\left.\frac{H_{c1}'(-)}{H_{c1}'(+)}\right|_{\mathbf{H}\parallel a}=\left(1+\frac{\beta_2}{\beta_1}\right)\left(\frac{3}{4}+\frac{1}{4}\frac{\kappa_1}{\kappa_{123}}\right), \tag{3}$$

$$R_b=\left.\frac{H_{c1}'(-)}{H_{c1}'(+)}\right|_{\mathbf{H}\parallel b}=\left(1+\frac{\beta_2}{\beta_1}\right)\left(\frac{3}{4}+\frac{1}{4}\frac{\kappa_{123}}{\kappa_1}\right), \tag{4}$$

and

$$R_c=\left.\frac{H_{c1}'(-)}{H_{c1}'(+)}\right|_{\mathbf{H}\parallel c}=\left(1+\frac{\beta_2}{\beta_1}\right)\frac{(\kappa_1+\kappa_{123})^2}{4\kappa_1\kappa_{123}}, \tag{5}$$

where R_a, R_b, and R_c represents respectively the slope ratios for $\mathbf{H}\parallel a$, $\mathbf{H}\parallel b$, and $\mathbf{H}\parallel c$. The coupling strength between the symmetry-breaking field and the superconducting order parameter is given by

$$\frac{\epsilon}{\alpha_0}=\tfrac{1}{2}(T_c^+ - T_c^-). \tag{6}$$

Here T_c^+, T_c^-, T_H, and T_c^* are defined as in the HTS model. T_c^+ is the zero-field transition temperature; T_c^* is the temperature of the lower heat-capacity jump and of the kink in H_{c1}; T_c^- is related to the position of the kink in H_{c2} (which is called T_H) by extrapolation of the H_{c2} curve to zero field (see Fig. 3).

Another component of the HTS model is the presence of an anomaly in H_{c2} for the field in the basal plane, which is expected to be absent for $\mathbf{H}\parallel c$. H_{c2} measurements for all three orientations were performed on a needle-shaped specimen (with the dimension of 0.08 $\times 0.08\times 2.76$ mm^3) spark cut from the *same* UPt_3 ingot using the conventional four-wire ac resistivity technique. For $\mathbf{H}$ parallel to the a and b axes, the upper-critical-field measurements were repeated with the sample cooled to 1 K in a field of 1 T, first applied at temperatures above 10 K. The field was then ramped to zero, prior to further cooling and initiating the critical-field measurements. The latter procedure was used because an antiferromagnetic (AFM) ordering with $T_N\sim 5.0$ K has been observed for UPt_3 in neutron diffraction experiments.[7] With a 1-T field cooling, the $\mathbf{q}$ vector associated with the AFM phase is presumably "locked" perpendicular to the field in the basal plane. We were curious to see if any difference in the upper critical fields could be observed with and without the field cooling.

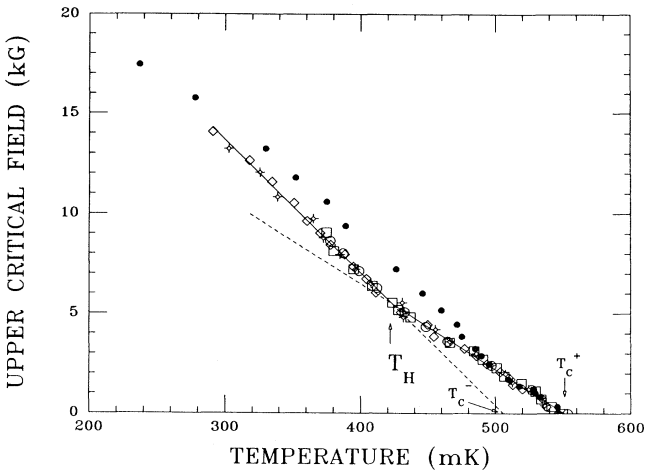

FIG. 3. The upper critical field vs temperature: ◇ (✧) represent data taken with the field along the a axis with (without) the $\mathbf{q}$-vector locking field; ○ (□) represent data taken with the field along the b axis with (without) the $\mathbf{q}$-vector locking field; ● represent data taken with the field parallel to the c axis. The solid lines are the linear least-squares fits of the $\mathbf{H}\perp c$-axis data and the dashed lines are extrapolations.

The measured upper-critical-field results are plotted in Fig. 3. We note the following: (1) No difference in the upper critical field is observed with or without field cooling. (2) A distinct slope change is observed with $\mathbf{H}\perp c$, yielding $T_H=420$ mK, $T_c^+=551$ mK, and $T_c^-=506$ mK. The relation between them (from the HTS model) is given by

$$T_H=\frac{T_c^- - T_c^+(1+\kappa_{23}/\kappa_1)^{1/2}}{1-(1+\kappa_{23}/\kappa_1)^{1/2}}. \tag{7}$$

The $\mathbf{H}\parallel c$ data (solid circles) show more curvature at a temperature close to T_c, and possibly a kink or an inflection point at $T\simeq 0.5$ K. The HTS model predicts no such features. Using the measured parameters (T_c^*, T_H, T_c^+, and T_c^-), with Eqs. (2), (6), and (7), one obtains the Landau-Ginzburg parameters $\beta_2/\beta_1=0.17$, $\kappa_{23}/\kappa_1=-0.58$ (the nonzero value of κ_{23} is not consistent with our observation that $R_a=R_b$), and the coupling strength $\epsilon/\alpha_0=23$ mK, which are quite close to the results of some other groups.[10,13]

In conclusion, we have performed comprehensive measurements of the lower and upper critical fields of UPt_3 for all orientations. A kink in the lower critical field has been observed at 392 ± 4 mK for all principal magnetic-field

orientations on a single spherical sample. This feature is in agreement with the predictions of a model by Hess, Tokuyasu, and Sauls. Together with the anomalies in H_{c2} and heat capacity (all performed on samples from the same ingot), this yields further evidence for unconventional superconductivity in UPt_3. The lower critical fields are anisotropic at temperatures below 290 mK being lower for fields along the c axis than for the basal plane. *No* anisotropy has been observed in the basal plane, and therefore $R_a = R_b$. Our measurements of the upper critical field show no difference with and without field locking of the AFM ordering.

The authors would like to thank D. Hess, T. A. Tokuyasu, J. A. Sauls, and S. K. Yip for many useful discussions. This work was supported by the National Science Foundation under Grant No. DMR-89-07396. The Low Temperature Laboratory receives support from the Northwestern Materials Research Laboratory under NSF Grant No. DMR-0830-520-H762.

---

*Permanent address: Department of Physics, University of Wisconsin at Parkside, Kenosha, WI 53141.

[1]Y. J. Qian, M-F. Xu, A. Schenstrom, H. P. Baum, J. B. Ketterson, D. Hinks, M. Levy, and B. K. Sarma, Solid State Commun. **63**, 599 (1987).

[2]V. Müller, Ch. Roth, D. Maurer, E. W. Scheidt, K. Lüders, E. Bucher, and H. E. Bömmel, Phys. Rev. Lett. **58**, 1224 (1987).

[3]A. Schenstrom, M-F. Xu, Y. Hong, D. Bein, M. Levy, B. K. Sarma, S. Adenwalla, Z. Zhao, T. Tokuyasu, D. W. Hess, J. B. Ketterson, J. A. Sauls, and D. G. Hinks, Phys. Rev. Lett. **62**, 332 (1989).

[4]R. N. Kleiman, P. L. Gammel, E. Bücher, and D. J. Bishop, Phys. Rev. Lett. **62**, 328 (1989).

[5]R. A. Fisher, S. Kim, B. F. Woodfield, N. E. Phillips, L. Taillefer, K. Hasselbach, J. Flouquet, A. L. Giorgi, and J. L. Smith, Phys. Rev. Lett. **62**, 1411 (1989).

[6]K. Hasselbach, L. Taillefer, and J. Flouquet, Phys. Rev. Lett. **63**, 93 (1989).

[7]G. Aeppli, E. Bucher, C. Broholm, J. K. Kjems, J. Baumann, and J. Hufnagl, Phys. Rev. Lett. **60**, 615 (1988).

[8]S. Adenwalla, S. W. Lin, Q. Z. Ran, Z. Zhao, J. B. Ketterson, J. A. Sauls, L. Taillefer, D. G. Hinks, M. Levy, and B. K. Sarma, Phys. Rev. Lett. **65**, 2298 (1990).

[9]D. W. Hess, T. A. Tokuyasu, and J. A. Sauls, J. Phys. Condens. Matter **1**, 8135 (1989).

[10]B. S. Shivaram, J. J. Gannon, Jr., and D. G. Hinks, Phys. Rev. Lett. **63**, 1723 (1989).

[11]F. Behroozi, Am. J. Phys. **51**, 28 (1983).

[12]E. Vincent, J. Hammann, L. Taillefer, K. Behnia, N. Keller, and J. Flouquet (unpublished).

[13]L. Taillefer, F. Piquemal, and J. Flouquet, Physica C **153-155**, 451 (1988).